

CAHN-HILLIARD VS SINGULAR CAHN-HILLIARD EQUATIONS IN SIMULATIONS OF IMMISCIBLE BINARY FLUIDS*

Lizhen Chen

Abstract An efficient semi-implicit spectral method is implemented to solve the Cahn-Hilliard equation with a variable mobility in this paper. We compared the kinetics of bulk-diffusion-dominated and interface-diffusion-dominated coarsening in two-phase systems. As expected, the interface-diffusion-controlled coarsening evolves much slower. Also we find that the velocity field will be caused different greatly by using Singular Cahn-Hilliard equation and using Cahn-Hilliard in the simulation of immiscible binary fluids.

Keywords Cahn-Hilliard equations, singular, immiscible binary fluids.

MSC(2010) 65M06, 65M12, 65N30, 65N35, 76A05.

1. Introduction

The Cahn-Hilliard (CH) equation is originally introduced by Cahn-Hilliard [6] in 1958 to describe the phase separation and coarsening phenomena in glass and polymer systems. Now it used to model many moving interface problems from fluid dynamics to materials science through a phase-field approach (see, for instance, [2, 7, 8, 10, 20, 22, 24, 25]).

There have been many existing simulations using a CH equation employing a constant mobility, corresponding to bulk-diffusion-dominated coarsening [4, 9, 17, 18, 20, 23] and the reference therein. Finite element schemes have been studied with mathematical rigor, see, e.g., [3, 12–15]. Finite difference approaches were proposed to solve the Cahn-Hilliard equation in [5, 16]. In [17], a combined spectral and large-time stepping method was proposed and studied for the Cahn-Hilliard equation which can increase the time-step size a few times larger when the the equation involving a small constant mobility.

However, there have been very few studies of the effect of a variable mobility on the coarsening kinetics of a two-phase system. Lacasta et al. give the direct numerical solution of a Cahn-Hilliard equation with a variable mobility, and showed a significant effect of composition dependence of the mobility on the coarsening kinetics of a two-phase mixture [1, 19]. More recently, Bray et al. derived a growth

Email address: lzchen@csrc.ac.cn (L. Chen)

Beijing Computational Science Research Center, Beijing 100193, China

*The author was supported by National Natural Science Foundation of China through Grants (11671166, U1530401) and Postdoctoral Science Foundation of China (2015M580038).

law corresponding to the CH equation with variable mobility, in the Lifshitz-Slyozov limit where the minority phase occupies a vanishingly small volume fraction [11].

As we known, the singular Cahn-Hilliard equation tends to annihilate dissipation and mixing outside the interfacial layer, therefore it is more physically relevant to the interfacial problem. The main purpose of this paper is propose an efficient semi-implicit spectral method to the singular Cahn-Hilliard equation. In order to improve the stability, two stability terms are added to the time discretization scheme. Furthermore, we will compare the numerical simulations of immiscible binary fluids by the Cahn-hilliard equation with constant mobility and variable mobility.

This paper is organized as follows. In the next section, we introduce two phase field model for the mixture of two incompressible fluids with CH and SCH equation respectively. In Section 3, we present the numerical schemes with respect to time and space discretization. We present in Section 4 some numerical experiments. It demonstrated that the interface-diffusion-controlled coarsening evolves much slower than the bulk-diffusion-dominated coarsening evolves, also sometimes it would caused different evolves. Some concluding remarks are given in the final section.

2. The mathematical model

Consider the following non-dimensional system modeling a specific type of mixture of two incompressible fluids with same density (which is taken to be 1) and same viscosity constants [21]:

$$\begin{aligned} \frac{\partial \mathbf{u}}{\partial t} + \mathbf{u} \cdot \nabla \mathbf{u} + \nabla p - \nu \operatorname{div} D(\mathbf{u}) + \lambda \nabla \cdot (\nabla \phi \otimes \nabla \phi) &= \mathbf{0}, \\ \nabla \cdot \mathbf{u} &= 0, \end{aligned} \quad (2.1)$$

$$\frac{\partial \phi}{\partial t} + (\mathbf{u} \cdot \nabla) \phi + \nabla \cdot \left(\gamma(\phi) \nabla \frac{\delta E(\phi)}{\delta \phi} \right) = 0, \quad (\mathbf{x}, t) \in \Omega \times (0, T), \quad (2.2)$$

with initial conditions

$$\mathbf{u}(\mathbf{x}, 0) = \mathbf{0}, \quad \phi(\mathbf{x}, 0) = \phi_0(\mathbf{x}), \quad \mathbf{x} \in \Omega, \quad (2.3)$$

and periodic boundary conditions.

In the above system, \mathbf{u} represents the velocity vector of the fluids, p is the pressure, ϕ represents the "phase" of the molecules, ν is the viscosity constant, and λ corresponds to the surface tension [21]. $\Omega = (0, L_1) \times (0, L_2)$, $\phi_0 : \Omega \rightarrow \mathbb{R}$ is a given initial function.

$\gamma(\phi)$ is a nonnegative function, when $\gamma(\phi) = 1$, the above Cahn-Hilliard equation with constant mobility, describing the dynamics controlled by bulk diffusion. When $\gamma(\phi) = 1 - \phi^2$ (Singular Cahn-Hilliard equation), the bulk diffusion is severely reduced, which corresponds to the interface-diffusion-controlled dynamics, i.e., the coarsening process is mainly due to the diffusion along the interface between the two phases.

Finally, $E(\phi)$ is the free energy function defined by:

$$E(\phi) = \int_{\Omega} \left[\gamma_1 \frac{1}{2} |\nabla \phi|^2 + \gamma_2 F(\phi) \right] dx, \quad (2.4)$$

where γ_1 and γ_2 are parameters parametrizing the strength of the bulk energy and conformational entropy, respectively. And

$$F(\phi) = \frac{(\phi^2 - 1)^2}{4\eta^2} \quad (2.5)$$

is the bulk part of the mixing energy with η as the capillary width (width of the mixing layer).

3. Numerical scheme

In this section, we shall focus on constructing efficient and easy to implement numerical schemes.

3.1. Discretization in time

In what follows, the superscript n denotes the time step level and Δt is the time step size. Now we will present the time discretization of the mathematical model (2.1)-(2.2) with Cahn-Hilliard equation and Singular Cahn-Hilliard equation respectively.

We impsd a second-order semi-implicit time discretization scheme for (2.1).

$$\begin{aligned} & \frac{4\mathbf{u}^{n+1} - 3\mathbf{u}^n + \mathbf{u}^{n-1}}{2\Delta t} + 2\mathbf{u}^n \cdot \nabla \mathbf{u}^n - \mathbf{u}^{n-1} \cdot \nabla \mathbf{u}^{n-1} + \nabla p^{n+1} \\ & - \nu \operatorname{div} D(\mathbf{u}^{n+1}) + 2\lambda \nabla \cdot (\nabla \phi^n \otimes \nabla \phi^n) - \lambda \nabla \cdot (\nabla \phi^{n-1} \otimes \nabla \phi^{n-1}) = 0, \\ & \nabla \cdot \mathbf{u}^{n+1} = 0, \end{aligned}$$

And second-order semi-implicit time discretization scheme for (2.2) when $\gamma(\phi) = 1$:

$$\begin{aligned} & \frac{4\phi^{n+1} - 3\phi^n + \phi^{n-1}}{2\Delta t} + \gamma_1 \Delta^2 \phi^{n+1} - s_2 \gamma_2 \Delta(\phi^{n+1} - 2\phi^n + \phi^{n-1}) \\ & + 2\Delta \frac{\delta F(\phi^n)}{\delta \phi} - \Delta \frac{\delta F(\phi^{n-1})}{\delta \phi} = 0, \end{aligned} \quad (3.1)$$

first-order semi-implicit time discretization scheme for (2.2) when $\gamma(\phi) = 1 - \phi^2$:

$$\frac{\phi^{n+1} - \phi^n}{\Delta t} + s_1 \gamma_1 \Delta^2 (\phi^{n+1} - \phi^n) - s_2 \gamma_2 \Delta (\phi^{n+1} - \phi^n) + \nabla \cdot ((1 - (\phi^n)^2) \nabla \frac{\delta E(\phi^n)}{\delta \phi}) = 0, \quad (3.2)$$

where s_1 and s_2 are positive constants. Here, we have added a extra stability term $s_2 \gamma_2 \Delta (\phi^{n+1} - 2\phi^n + \phi^{n-1})$ which of order $\mathcal{O}(\Delta t^2 \partial_{tt} \phi)$ in (3.1) and two extra stability terms $s_1 \gamma_1 \Delta^2 (\phi^{n+1} - \phi^n)$ and $s_2 \gamma_2 \Delta (\phi^{n+1} - \phi^n)$ which both of order $\mathcal{O}(\Delta t \partial_t \phi)$ in (3.2).

A complete stability and error analysis for the above scheme is beyond the scope of this paper whose main purpose is to propose and justify a phase field model for the mixture of two incompressible fluids. The adding of the stability terms $s_2 \gamma_2 \Delta (\phi^{n+1} - 2\phi^n + \phi^{n-1})$ and $s_2 \gamma_2 \Delta (\phi^{n+1} - \phi^n)$ have been discussed before [17, 20]. Nevertheless, we will give a test to research the sensitive of value s_1 .

3.2. Discretization in space

A complete numerical algorithm also requires a discretization strategy in space. Since Fourier spectral method is one of the most suitable spatial approximation methods for periodic problems, it will be employed to handle the spatial discretization on two-dimensional fluid flows in both drop dynamics as well as mixing dynamics of immiscible binary fluids. We use the following Fourier basis functions:

$$\mathbb{P}_M = \text{span}\{1, \sin nx, \cos nx, n = 1, \dots, N\} \times \text{span}\{1, \sin my, \cos my, m = 1, \dots, M\}, \quad (3.3)$$

The spatial discretization is based on a Fourier pseudospectral approximation with N and M denoting the number of the Fourier mode.

4. Numerical results and discussions

Below, we present several numerical experiments using this code. In all computations, we have fixed the physical parameters to be

$$\eta = 0.02, \lambda = 0.1, \nu = 0.1, \gamma_1 = 0.1, \gamma_2 = 0.1,$$

and the computational parameters to be

$$s_1 = 0.5, s_2 = 2, N = 256, \Delta t = 0.0001.$$

We use a phase variable ϕ to label each fluid Fig.1:

$$\phi = \begin{cases} 1, & \text{in fluid 1;} \\ -1, & \text{in fluid 2.} \end{cases} \quad (4.1)$$

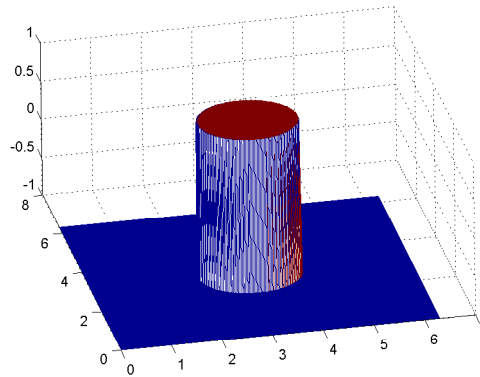


Figure 1. Phase variable ϕ .

Example 4.1. We start with two kissing bubbles (fluid 1). It is observed that the two bubbles coalesce into one big bubble as time evolves from Fig.2 and Fig.3 which the CH and SCH is used respectively. This is the combination of the surface tension effect and the elastic effect from the phase equation.

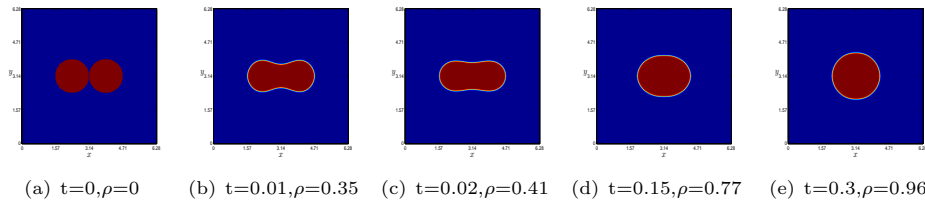


Figure 2. Contour plots of two kissing droplets at selected time slots, where the CH model is used.

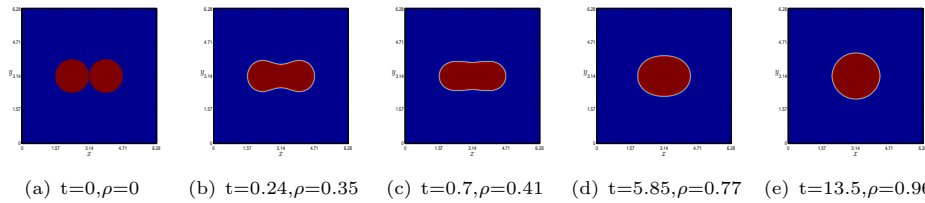


Figure 3. Contour plots of two kissing droplets at selected time slots, where the SCH model is used.

Let ρ to be the ratio of length in short axis and length in major axis. Fig.4 and Fig.5 display the velocity vector field, pressure image and phase contour at selected ρ slots, where the CH and SCH model is used respectively. It observed that the velocity vector field of this two model both lead to vortexes around the bubble, but the SCH model caused more stronger vortexes because of longer time evolved. Also we find that SCH model would take longer time to evolve the same formation of the bubble as the CH model. For example, it should take time 0.7 correspond to $\rho = 0.41$ when SCH model is used as the 0.02 when CH model is used.

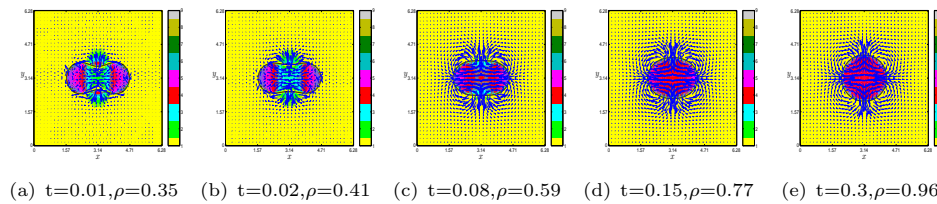


Figure 4. Velocity vector field, pressure image and phase contour, where the CH model is used.

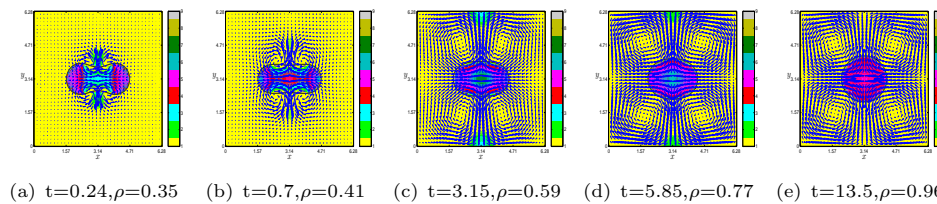


Figure 5. Velocity vector field, pressure image and phase contour, where the SCH model is used.

To compare the evolution speed of this two models, we plot the ρ versus t in Fig.6 between $[0, 10]$ and Fig.7 between $[0, 1]$ using the CH and SCH model, also with different s_1 in SCH model. It takes about 0.4 (Fig.7) to finish the complete

evolution with CH model, but more than 10 with SCH model (Fig.6). The SCH model coarsening evolves much slower than CH model. Fig.7 also illustrates that the time discrete scheme is not very sensitive with s_1 (which usually belong to $(0, 2]$) in this example.

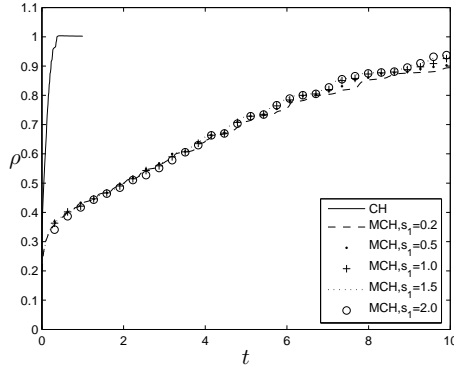


Figure 6. The process ρ versus t between $[0, 10]$ using the CH and SCH with different s_1 .

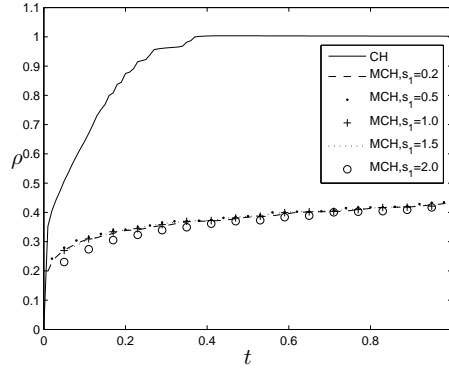


Figure 7. The process ρ versus t between $[0, 1]$ using the CH and SCH with different s_1 .

Example 4.2. Secondly, we simulate two droplets of fluid 1 of radius ratio 2 : 1 immersed in fluid 2 at selected time slots using the CH and SCH respectively. Notice that the small bubble is absorbed by the big bubble in both Fig.8 and Fig.9. This phenomenon, i.e., the mass in the smaller droplet is transported into the larger one is purely due to the Cahn-Hilliard equation, since the curvature of the bubbles serves as the chemical potential in the dynamics of the phase function.

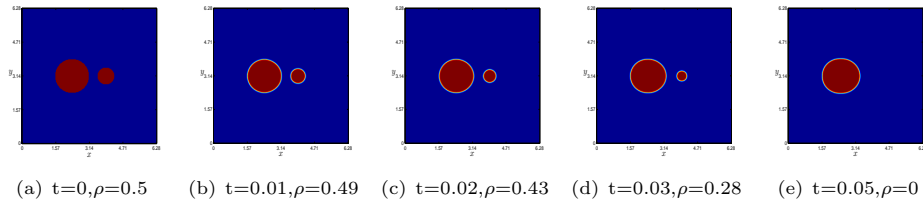


Figure 8. Contour plots of two droplets with initial radius ratio 2 : 1 at selected time slots, where the CH model is used.

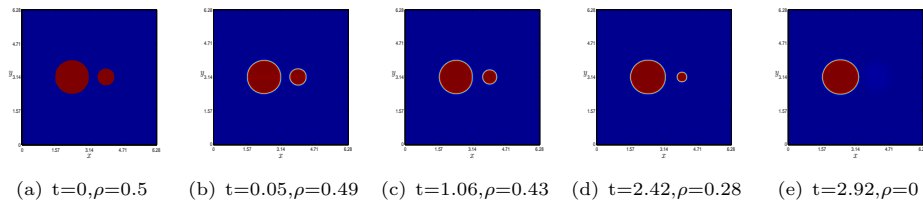
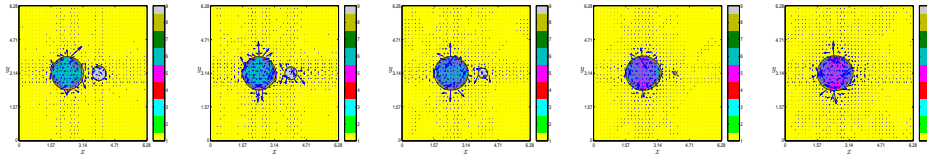


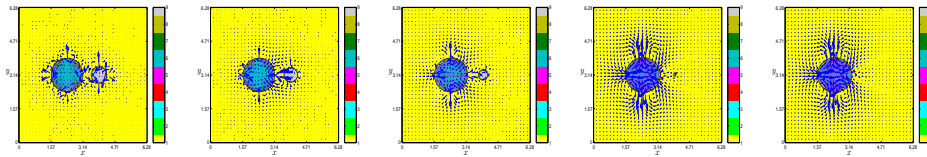
Figure 9. Contour plots of two droplets with initial radius ratio 2 : 1 at selected time slots, where the SCH model is used.

Define the ρ to be the ratio of the radius of the small droplet and the big

droplet. Velocity vector field, pressure image and phase contour at selected ρ slots corresponded to the CH and SCH model are presented in Fig.10 and Fig.11. Notice that the velocity vector field in Fig.10 do not have changed greatly at the end of evolution, but it causes some vertexes in Fig.11 which has much more longer time evolved. From Fig.12, we can conclude that the mass dissipation and volume-reduction in the smaller droplet with SCH model is much weaker than the CH model in the numerical experiment. It seems the time discrete scheme has little sensitive with s_1 but noticeable. Generally, we would like to chose s_1 equal to 0.5.



(a) $t=0.01, \rho=0.49$ (b) $t=0.02, \rho=0.43$ (c) $t=0.03, \rho=0.28$ (d) $t=0.04, \rho=0.08$ (e) $t=0.05, \rho=0$
Figure 10. Velocity vector field, pressure image and phase contour, where the CH model is used.



(a) $t=0.05, \rho=0.49$ (b) $t=1.06, \rho=0.43$ (c) $t=2.42, \rho=0.28$ (d) $t=2.91, \rho=0.08$ (e) $t=2.92, \rho=0$
Figure 11. Velocity vector field, pressure image and phase contour, where the SCH model is used.

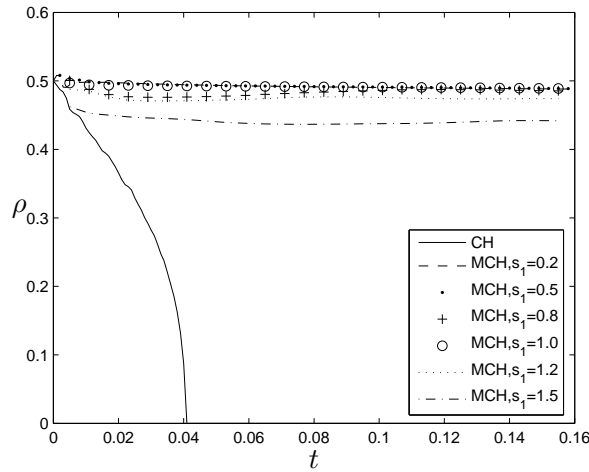


Figure 12. The process ρ versus t between $[0, 0.16]$ using the CH and SCH with different s_1 .

Example 4.3. In this example, we chose the physical parameter $\gamma_1 = \gamma_2 = 1$ in the SCH model, and $\gamma_1 = \gamma_2 = 0.1$ in the CH model. And we add a term $\nabla \mathbf{c}(\mathbf{x})$ to

the advection term of equation (2.2) as following:

$$\frac{\partial \phi}{\partial t} + \nabla \cdot (\mathbf{u} - \mathbf{c}(\mathbf{x}))\phi + \nabla \cdot (\gamma(\phi)\nabla \frac{\delta E(\phi)}{\delta \phi}) = 0, (\mathbf{x}, t) \in \Omega \times (0, T). \quad (4.2)$$

Firstly, we chose

$$\nabla \mathbf{c}(\mathbf{x}) = (2 \times (\tanh \frac{|x - \pi| - 0.5}{0.05} + 1), 0). \quad (4.3)$$

We plot the contour of one droplets at selected time slots in Fig.13 and Fig.15, where the CH and SCH model is used. One observes that the shape of bubble does not have change greatly except it shrinks as time delaying and move to the left when using CH model, by switching to the SCH, except the shrinking and moving a little, the shape of bubble have been changed and looks like crescent in the middle progress. Then presented in Fig.14 and Fig.16 the velocity vector field, pressure image and phase contour.

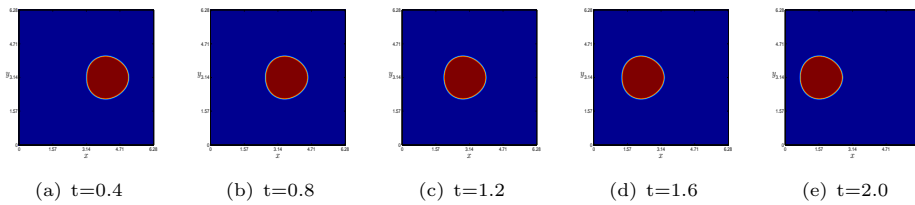


Figure 13. Contour plots of one droplets at selected time slots, where the CH model is used.

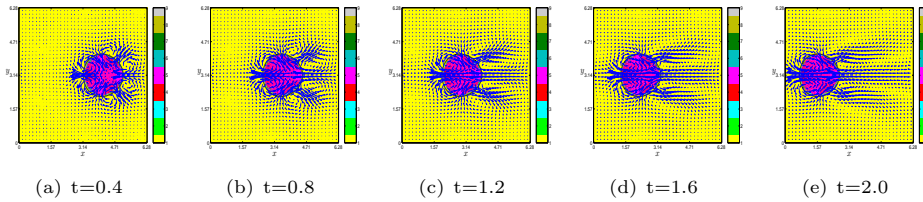


Figure 14. Velocity vector field, pressure image and phase contour, where the CH model is used.

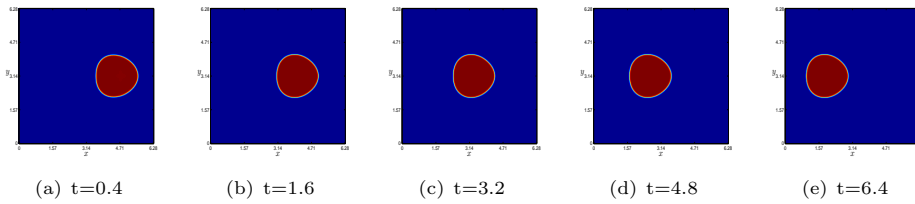


Figure 15. Contour plots of one droplets at selected time slots, where the SCH model is used.

Secondly, we chose

$$\nabla \mathbf{c}(\mathbf{x}) = (2 \times (\tanh \frac{|x - \pi| - 0.2}{0.05} + 1), 0). \quad (4.4)$$

Fig.17 and Fig.19 indicate contour of the droplet at selected time slots, where the CH and SCH model is used respectively, we find that the shape the droplet is

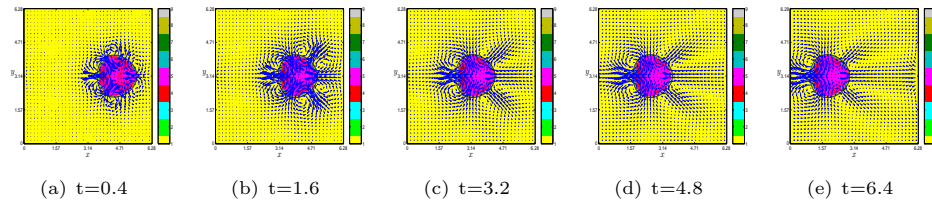


Figure 16. Velocity vector field, pressure image and phase contour, where the SCH model is used.

changed using SCH model much more than CH model. Then presented in Fig.14 and Fig.16 the velocity vector field, pressure image and phase contour. Velocity vector field, pressure image and phase contour was plotted in Fig.18 and Fig.20 .

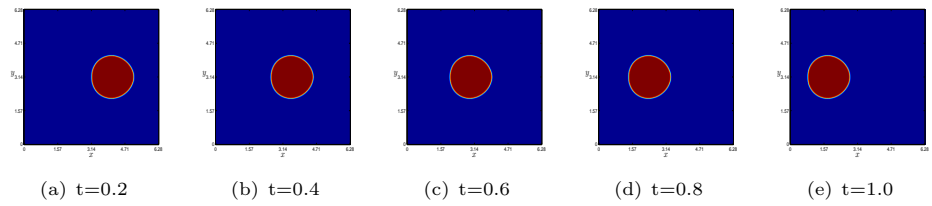


Figure 17. Contour plots of one droplet at selected time slots, where the CH model is used.

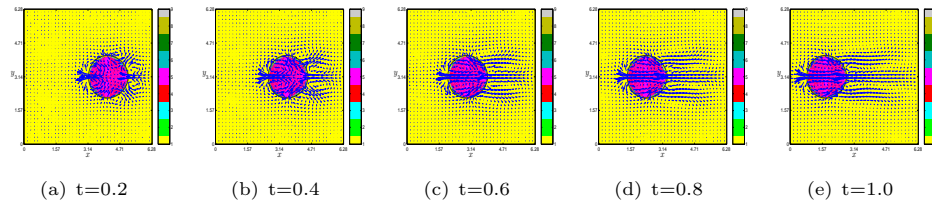


Figure 18. Velocity vector field, pressure image and phase contour, where the CH model is used.

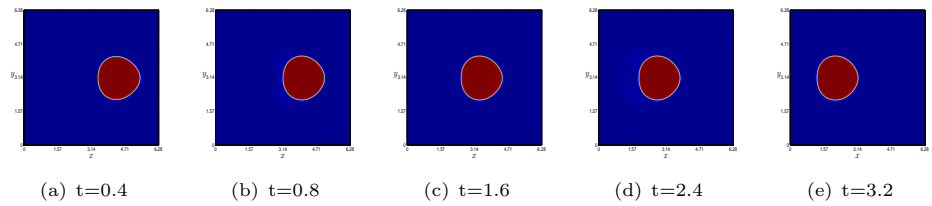


Figure 19. Contour plots of one droplets at selected time slots, where the SCH model is used.

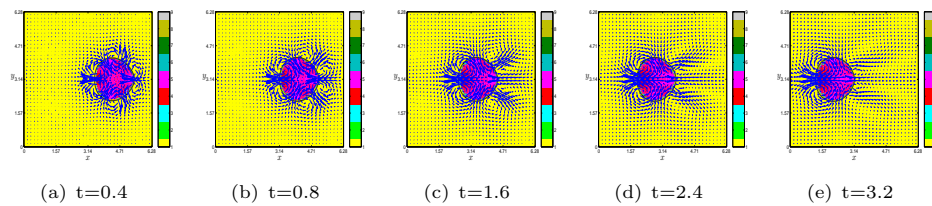


Figure 20. Velocity vector field, pressure image and phase contour, where the SCH model is used.

These simulation show that the SCH models clearly render much smaller numerical dissipation and give better resolution in the immiscible droplet simulation than the CH model.

5. Conclusion

In this paper, we compare the use of the Cahn-hilliard equation (of a constant mobility) for the phase variable with that of the singular or modified Cahn-Hilliard equation (of a variable mobility) in the context of physical derivation of the transport equation and numerical simulations of immiscible binary fluids. It was shown that the last model is more efficient and accurate, thus allowing us to work on large systems and for long times. In future, we would use the SCH equations in multi-phase flow simulations for immiscible fluids since this model certainly provide better numerical resolution and physical fidelity to the interface problem.

References

- [1] H. M. Aurora, R. Toral, A. M. Lacasta and J. M. Sancho, *Effects of domain morphology in phase-separation dynamics at low temperature*, Phys. Rev. B, 1993, 48, 6854–6857.
- [2] D. M. Anderson, G. B. McFadden and A. A. Wheeler, *Diffuse-interface methods in fluid mechanics*, 1998, 30, 139–165.
- [3] J. W. Barrett, J. F. Blowey and H. Garcke, *On fully practical finite element approximations of degenerate Cahn-Hilliard systems*, Math. Model. Numer. Anal., 2001, 35(4), 713–748.
- [4] A. Chakrabarti, R. Toral and J. D. Gunton, *Late-stage coarsening for off-critical quenches: Scaling functions and the growth law*, Phys. Rev. E, 1993, 47(5), 3025.
- [5] B. Costa, W. S. Don, D. Gottlieb and R. Sendersky, *Two-dimensional multi-domain hybrid spectral-WENO methods for conservation laws*, Commun. Comput. Phys., 2006, 1(3), 548–574.
- [6] J. W. Cahn and J. E. Hilliard, *Free energy of a nonuniform system I. Interfacial free energy*, J. Chem. Phys., 1958, 28, 258–267.
- [7] L. Q. Chen, *Phase-field models for microstructure evolution*, Annual Review of Material Research, 2002, 32, 113–140.
- [8] L. Q. Chen and J. Shen, *Applications of semi-implicit Fourier-spectral method to phase-field equations*, Comput. Phys. Comm., 1998, 108, 147–158.
- [9] Q. Du, B. Y. Guo and J. Shen, *Fourier spectral approximation to a dissipative system modeling the flow of liquid crystals*, SIAM J. Numer. Anal., 2002, 39(3), 735–762.
- [10] Q. Du, C. Liu and X. Wang, *Simulating the deformation of vesicle membranes under elastic bending energy in three dimensions*, J. Comput. Phys, 2005, 212, 757–777.
- [11] C. L. Emmott and A. J. Bray, *Lifshitz-Slyozov scaling for late-stage coarsening with an order-parameter-dependent mobility*, Phys. Rev. B, 1995, 52(2), 685–688.

- [12] C. M. Elliott and S. Larsson, *Error estimates with smooth and nonsmooth data for a finite element method for the Cahn-Hilliard equation*, Math. Comput., 1992, 58(198), 603–630.
- [13] C. M. Elliott and Z. Songmu, *On the Cahn-Hilliard equation*, Arch. Rational Mech. Anal., 1986, 96(4), 339–357.
- [14] D. A. French and C. M. Elliott, *Numerical studies of the Cahn-Hilliard equation for phase separation*, IMA Journal of Applied Mathematics, 1987, 38(2), 97–128.
- [15] D. A. French and C. M. Elliott, *A nonconforming finite-element method for the two-dimensional Cahn-Hilliard equation*, SIAM J. Numer. Anal., 1989, 26(4), 884–903.
- [16] D. Furihata, *A stable and conservative finite difference scheme for the Cahn-Hilliard equation*, Numer. Math., 2001, 87(4), 675–699.
- [17] Y. N. He, Y. X. Liu and T. Tang, *On large time-stepping methods for the cahn-hilliard equation*, Appl. Numer. Math., 2007, 57(5), 616–628.
- [18] T. Küpper and N. Masbaum, *Simulation of particle growth and ostwald ripening via the cahn-hilliard equation*, Acta metallurgica et materialia, 1994, 42(6), 1847–1858.
- [19] A. M. Lacasta, A. Hernández-Machado, J. M. Sancho and R. Toral, *Domain growth in binary mixtures at low temperatures*, Phys. Rev. B, 1992, 45, 5276–5281.
- [20] C. Liu and J. Shen, *A phase field model for the mixture of two incompressible fluids and its approximation by a Fourier-spectral method*, Physica D, 2003, 179(3), 211–228.
- [21] C. Liu and N. J. Walkington, *An Eulerian description of fluids containing visco-elastic particles*, Arch. Rational Mech. Anal., 2001, 159(3), 229–252.
- [22] J. Lowengrub and L. Truskinovsky, *Quasi-incompressible cahn-hilliard fluids and topological transitions*, Proc. R. Soc. Lond. A, 1998, 454, 2617–2654.
- [23] T. M. Rogers and R. C. Desai, *Numerical study of late-stage coarsening for off-critical quenches in the cahn-hilliard equation of phase separation*, Phys. Rev. B, 1989, 39(16), 11956.
- [24] X. Yang, J. J. Feng, C. Liu and J. Shen, *Numerical simulations of jet pinching-off and drop formation using an energetic variational phase-field method*, J. Comput. Phys., 2006, 218, 417–428.
- [25] P. Yue, J. J. Feng, C. Liu and J. Shen, *A diffuse-interface method for simulating two-phase flows of complex fluids*, J. Fluid Mech., 2004, 515, 293–317.